Interactions of 4-Nitroquinoline 1-Oxide with Deoxyribodinucleotides[†]

Stephen A. Winkle* and Ignacio Tinoco, Jr.

ABSTRACT: The interactions of 4-nitroquinoline 1-oxide (NQO), a potent mutagen and carcinogen, with several self- and non-self-complementary deoxydinucleotides were probed by using absorption spectra of the charge transfer bands and ^{1}H and ^{13}C NMR spectra. Absorption spectra were analyzed by using Benesi–Hildebrand-type equations to yield stoichiometries and equilibrium constants of complex formation. Non-self-complementary dimers form weak 1:1 complexes [dpTpG:NQO, K(25 °C) = 22 M^{-1}] while self-complementary dimers form strong 2:1 complexes [(dpCpG)$_2$:NQO, K(25 °C) = 2.2 × 10^4 M^{-2}]. A mixture of dpTpG and dpCpA with NQO gives a 2:1 complex [dpTpG:NQO:dpCpA, K(25 °C) = 8.6 × 10^3 M^{-2}]. Analyses of the changes in ^{13}C and ^{1}H NMR chemical shifts with complex formation gave approximate orientations for the intercalation of NQO with self-complementary dimer minihelixes. In the (dpCpG)$_2$:NQO and (dpGpC)$_2$:NQO complexes, the NO$_2$ group of NQO probably lies in the major grove and the NO$_2$, NO containing NQO ring is stacked near the purine imidazole ring. In the (dpTpA)$_2$:NQO and (dpApT)$_2$NQO complexes, the NO$_2$ seems to project into the minor grove and the NQO benzenoid ring is over the purine imidazole ring.

The carcinogen and mutagen 4-nitroquinoline 1-oxide (NQO)[1] has been previously shown to interact with DNA so as to stack with the bases and to form charge-transfer complexes (Nagata et al., 1966; Okano et al., 1969a–c). Okano and co-workers used absorption spectra of the charge-transfer interactions to determine equilibrium constants for 1:1 deoxynucleoside:NQO complex formation (Okano et al., 1969b). In a previous paper (Winkle & Tinoco, 1978), we discussed the 1:1 complexes of 5′-deoxynucleotides and NQO. The charge-transfer absorption spectra were analyzed by using a form of the Benesi–Hildebrand equation (Benesi & Hildebrand, 1949) to yield equilibrium constants. The values of the equilibrium constants suggested a preference of NQO for binding to purine bases, supporting the earlier finding for deoxynucleosides of Okano et al. (1969b). Further, the equilibrium constants for deoxynucleotides were similar to those of the deoxynucleosides, showing that the presence of the phosphate group in the 5′ position has little effect on complex formation.

In the same paper we discussed possible structures of dpG:NQO and dpA:NQO complexes, obtained from ^{1}H and ^{13}C NMR of deoxynucleotide–NQO mixtures. In the dpG:NQO complex, the nitro *N*-oxide ring of NQO is positioned over the imidazole ring of the guanine base, with the nitro group projected toward the carbonyl of the guanine. In the dpA:NQO complex, it is the benzenoid ring of NQO which is over the imidazole ring of the adenine.

We now present the results of studies with NQO and deoxydinucleotides. The charge-transfer band spectra were analyzed with various Benesi–Hildebrand-type equations to obtain equilibrium constants and complex stoichiometries for both self-complementary and non-self-complementary dinucleotides. Through ^{1}H and ^{13}C NMR studies, possible geometries for the 2:1 complexes of the self-complementary deoxydinucleotides and NQO were obtained.

Materials and Methods

The deoxydinucleotides dpCpG, dpGpC, dpTpA, dpApT, dpTpG, and dpCpA were obtained from Collaborative Research. The NQO was synthesized from quinoline 1-oxide (Aldrich Chemical Co.) using the procedure of Ochiai (1953) and was recrystallized 3 times from hot acetone.

Optical studies were done in a buffer consisting of 0.1 M NaCl, 0.01 M sodium cacodylate, and 0.2 mM EDTA, pH 7.0. Concentrations of the deoxydinucleotide and NQO solutions were measured by using the absorbance at λ_{max}. A molar absorptivity for NQO of ϵ_{250} = 1.65 × 10^4 M^{-1} cm^{-1} was used (Okano et al., 1973). For the deoxydinucleotides, the values of ϵ_{max} for the dinucleoside phosphates were used (P. L. Biochemicals Reference and Price Guide 104). Glass tuberculin syringes were used for the measurement of nu-

[1] Abbreviations used: NQO, 4-nitroquinoline 1-oxide; DSS, 3-(trimethylsilyl)propanesulfonic acid.

cleotide and NQO solution volumes. Samples for the optical studies were prepared by placing a fixed volume of stock NQO solution in each sample tube ([NQO] ranged from 3.3×10^{-4} to 6.7×10^{-4} M), adding a given volume of the stock nucleotide solution ([dpN_1pN_2] ranged from 2.3×10^{-3} to 1.8×10^{-2} M) and then adding sufficient cacodylate buffer to produce a constant volume. The mixed deoxydinucleotide solutions had approximately equal concentrations of the two dinucleotides. Absorption spectra in the region of the complex band (460–380 nm) were recorded for each deoxydinucleotide–NQO mixture vs. a solution of equal NQO concentration to produce difference spectra. Absorption spectra were recorded at 25 °C on a Cary 118 spectrometer. Either 1.0- or 0.20-cm path length cells were used. The $\epsilon(dpN_1pN_2)$ values at the wavelength of the complex were obtained by measuring the absorption at this wavelength of nucleotide solutions in concentrations similar to those for the dpN_1pN_2–NQO mixtures.

For the ^{13}C NMR studies, the initial sample used consisted of $\sim$25 mL of a dinucleotide solution (concentration $\sim$4 $\times$ 10^{-3} M) in the pH 7 cacodylate buffer made up in 25–30% D_2O. After obtaining ^{13}C NMR spectra of the pure dinucleotide samples, $\sim$25 mL of an NQO solution in D_2O was added to each sample. The resulting solution was concentrated by using a rotary evaporator to the volume of the original dinucleotide solutions, making [NQO] $\sim$2 $\times$ 10^{-3} M. Successive samples were made by adding a small volume, usually 0.250 mL, of a concentrated dinucleotide stock solution in the cacodylate buffer to the dinucleotide–NQO solution. Thus, [dpN_1pN_2] ranged from about 4×10^{-3} to 6×10^{-3} M. The ^{13}C NMR spectra were obtained in a 25-mm probe at 45.3 MHz using a Bruker 180-MHz magnet and a Nicolet 1180 computer system. Samples were measured at 35 °C by using a 60° pulse with a 10-s delay, with broad-band proton decoupling, and with quadrature phase detection. About 8000–10 000 transients were collected for each sample. Samples were referenced to DSS (0.000 ppm). The spectral width was 9000 Hz with 16K data points to obtain 1-Hz resolution.

The ^{1}H NMR samples were prepared in a manner similar to that used for the optical studies. The appropriate amounts of dinucleotide solution in cacodylate buffer, NQO solution in cacodylate buffer, and cacodylate buffer were combined. The resulting mixture was lyophilized and reconstituted with D_2O. Total sample volume was 0.500 mL, [dpN_1pN_2] ranged from 1.2×10^{-2} to 2×10^{-3} mM, and [NQO] was $\sim$2 $\times$ 10^{-3} M. The ^{1}H NMR spectra were measured at 180.09 MHz by using the Bruker 180-MHz magnet and the Nicolet 1180 computer system. Measurements were made at 25 °C and referenced to DSS (0.000 ppm). The spectral width was 1800 Hz with 16K data points to obtain 0.2-Hz resolution.

Since NQO is a potent carcinogen and mutagen, all work with the solid compound, such as preparation of stock solutions, was done in a glovebox. Glassware was washed with special care, and all waste liquids and solid waste were collected for special disposal.

Results

The absorption spectra for the dinucleotide–NQO mixtures were difference spectra obtained by subtracting the NQO absorbances. All dinucleotide:NQO complex spectra displayed broad bands with maxima in the region 395–405 nm. The broad nature of the complex bands made it difficult to discern the exact complex λ_{max}. Hence, the absorbance at 400 nm of the dinucleotide–NQO samples was used for the optical studies.

In the case of a dinucleotide and NQO forming a 1:1 complex, the complex band absorption data should fit the equation developed for the mononucleotide–NQO mixtures (Winkle & Tinoco, 1978):

$$\frac{l[NQO]_T}{A_T - A_{dpN_1pN_2}} = \left(\frac{1}{K(\epsilon_c - \epsilon_{dpN_1pN_2} - \epsilon_{NQO})} \frac{1}{[dpN_1pN_2]_T} \right) + \frac{1}{\epsilon_c - \epsilon_{dpN_1pN_2} - \epsilon_{NQO}}$$

where [NQO]$_T$ and [dpN_1pN_2]$_T$ are the total NQO and dinucleotide concentrations, A_T and $A_{dpN_1pN_2}$ are the total absorbances of the sample at a given λ, ϵ_c, $\epsilon_{dpN_1pN_2}$, ϵ_{NQO} are the molar absorptivities of the complex, dinucleotide, and NQO at the λ used, l is the cell path length, and K is the equilibrium constant. For the case of a 2:1 dinucleotide:NQO complex, a similar equation may be derived.

$$\frac{l[NQO]_T}{A_T - A_{dpN_1pN_2}} = \left(\frac{1}{K(\epsilon_c - 2\epsilon_{dpN_1pN_2} - \epsilon_{NQO})} \frac{1}{[dpN_1pN_2]_T^2} \right) + \frac{1}{\epsilon_c - 2\epsilon_{dpN_1dpN_2} - \epsilon_{NQO}}$$

Such a 2:1 complex might be observed for a self-complementary dinucleotide–NQO mixture. With a mixture of two different dinucleotides and NQO, a 1:1:1 complex is possible with the data fitting the equation

$$\frac{l[NQO]_T}{A_T - A_{dpN_1pN_2} - A_{dpN_3pN_4}} = \left(\frac{1}{K(\epsilon_c - \epsilon_{dpN_1pN_2} - \epsilon_{dpN_3pN_4} - \epsilon_{NQO})} \times \frac{1}{x[dpN_1pN_2]_T[dpN_3pN_4]_T} \right) + \frac{1}{\epsilon_c - \epsilon_{dpN_1pN_2} - \epsilon_{dpN_3pN_4} - \epsilon_{NQO}}$$

To maintain the assumption implied in the above derivations, that [dpN_1pN_2]$_T$ $\gg$ [c], where [c] is the complex concentration, [dpN_1pN_2]$_T$ was always much larger than [NQO]$_T$. The quantity $A_{dpN_1pN_2}$ was calculated by using [dpN_1pN_2]$_T$ and the experimentally determined $\epsilon_{dpN_1pN_2}$ (at 400 nm). The values of $\epsilon_{dpN_1pN_2}$ at 400 nm ranged from 32.1 M^{-1} cm^{-1} for dpCpG to 5.8 M^{-1} cm^{-1} for dpTpG. These small absorbances (which are linear with [dpN_1pN_2]) are probably due to small amounts of impurities which become observable at the high nucleotide concentrations employed.

The plots of the absorption data for the different dinucleotide–NQO mixtures fitted to the equation giving best agreement are shown in Figure 1 (parts a–d). Data for two non-self-complementary dinucleotides, dpTpG and dpCpA, with NQO fit the 1:1 equation (Figure 1a). With the self-complementary dimers, dpCpG, dpGpC, dpTpA, and dpApT, the best fits were to the 2:1 equation (parts b and c of Figure 1). For a mixture of dpTpG and dpCpA with NQO, the data were fit to the 1:1:1 equation (Figure 1d). The equilibrium constants for the seven complexes obtained from these plots are presented in Table I. The molar absorptivities at 400 nm for the seven complexes, obtained from the same plots, are very
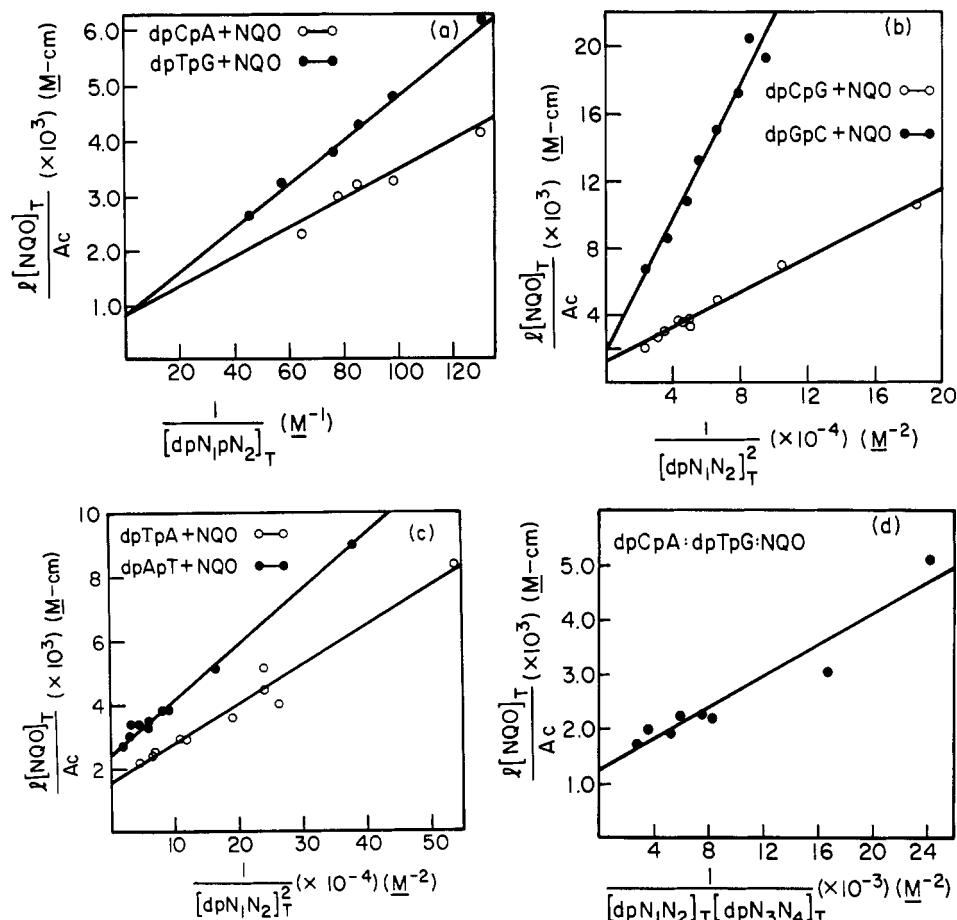
FIGURE 1: Benesi–Hildebrand-type plots of NQO:dinucleotide complex spectral data. (a) dpCpA (O), dpTpG (●); (b) dpCpG (O), dpGpC (●); (c) dpTpA (O), dpApT (●); (d) dpCpA + dpTpG. Temperature 25 °C; sodium cacodylate (0.01 M)–NaCl (0.1 M)–EDTA (0.2 mM) buffer, pH 7.0. Concentrations: $[NQO]_T = (3.3–6.7) \times 10^{-4}$ M; $[dpN_1pN_2]_T = 2.3 \times 10^{-3}–1.8 \times 10^{-2}$ M.

Table I: Equilibrium Constants at 25 °C for Deoxydinucleotide:Nitroquinoline Oxide Complex Formation

Noncomplementary Dinucleotides		Complementary Dinucleotides	
complex	$K(25 °C)$ $(M^{-1})^a$	complex	$K(25 °C)$ $(M^{-2})^b$
dpTpG:NQO	22	dpTpG:dpCpA:NQO	0.9×10^4
dpCpA:NQO	32	$(dpGpC)_2$:NQO	0.9×10^4
		$(dpTpA)_2$:NQO	1.3×10^4
		$(dpApT)_2$:NQO	1.4×10^4
		$(dpCpG)_2$:NQO	2.2×10^4

^{a} Maximum estimated error = ±5 M^{-1}. ^{b} Maximum estimated error = ±0.4 × 10^4 M^{-2}.

similar. Those for the four 2:1 and the one 1:1:1 complex equal 4100 ± 100 M^{-1} cm^{-1}, while the ϵ_c for the two 1:1 complexes equal 4700 ± 100 M^{-1} cm^{-1}.

The use of the large bore 25-mm probe in the ^{13}C NMR study permitted the observation of signals from dilute dinucleotide–NQO samples. The ^{13}C chemical shifts observed for the base carbons in dinucleotide–NQO mixtures are the weighted sums for the chemical shifts of the bound and various free states. We assume (as the ^{1}H NMR data suggest) that there is only one bound species. However, because of the lack of symmetry in the NQO molecule, in any 2:1 intercalation complex formed with self-complementary dinucleotides the two purine rings are affected differently by the NQO as are the two pyrimidines. Thus, the chemical shifts for each of the two purines (or pyrimidines) in the complex will be different. The chemical shift for a nucleus of a base in the bound species is the average of the shifts for the identical bases [$\delta_B = (\delta_{B1} +$

$\delta_{B2})/2$]. The value of δ_B for the base carbons in the 2:1 complex can be obtained from

$$\delta_B = \left(\delta_{obsd} - \frac{[dpN_1pN_2]_T - 2[c]}{[dpN_1pN_2]_T}\delta_F \right) \frac{[dpN_1pN_2]_T}{2[c]}$$
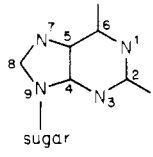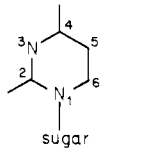
The complex concentrations, [c], were approximated by using the K values determined at 25 °C (Table I). The assignments of the free dinucleotide carbon signals, δ_F, will be discussed in a separate paper.

The δ_B values thus obtained for the carbons of the self-complementary dimers were used to calculate the differences (given in Table II) between δ_B and the chemical shifts, δ_M, of the appropriate mononucleotides. The δ_B values for the first base in the dimer, i.e., dpN$_1$– in the dimer dpN$_1$pN$_2$, are compared with δ_M values for the 5′-mononucleotide at pH 7. The δ_B values for –pN$_2$ are compared with the δ_M values for the 5′-mononucleotide at pH 5. In Table II, note that δ_B – δ_M < 0 represents chemical shift changes to *increasing* field strength (upfield).

The dinucleotide:NQO complexes of dPur-Pyr dinucleotides (dpGpC and dpApT) show ^{13}C shift changes which are mainly downfield, with the δ_B – δ_M values for (dpGpC)$_2$:NQO being larger, in general, than those for (dpApT)$_2$:NQO. Conversely, the dPyr-Pur dinucleotide complexes (involving dpCpG and dpTpA) have values for δ_B – δ_M which are either somewhat positive (slightly downfield) or negative (upfield changes). The specifics of the shift changes for each complex will be considered in the Discussion.

In the dpCpG–NQO and dpGpC–NQO mixtures, the dpN$_1$– C2′ (of the deoxyribose) resonance shifts notably

Table II: Differences in Average Carbon Chemical Shifts between Dimers Complexed with NQO and (Comparable) Free Mononucleotides[a]

purine (A, G)   pyrimidine (T, C)

$\delta_B - \delta_M$ (ppm)

dimer	C2	C4	C5	C6	G2	G4	G5	G6	G8
dpCpG	−0.75	−3.84	+0.12	−0.58	+1.54	−1.32	−1.40	−1.85	−1.40
dpGpC	+1.85	+3.38	+0.48	+0.75	+1.05	+1.54	+1.97	+1.11	+1.51

$\delta_B - \delta_M$ (ppm)

dimer	T2	T4	T5	T6	A2	A4	A5	A6	A8
dpTpA	−0.51	−0.37	+0.24	−0.53	+0.18	−0.32	−0.91	−0.45	−0.97
dpApT	+1.68	b	+0.04	+0.07	−1.58	+0.39	−0.55	b	+0.12

[a] Positive shift changes are downfield changes. [b] Not observable.

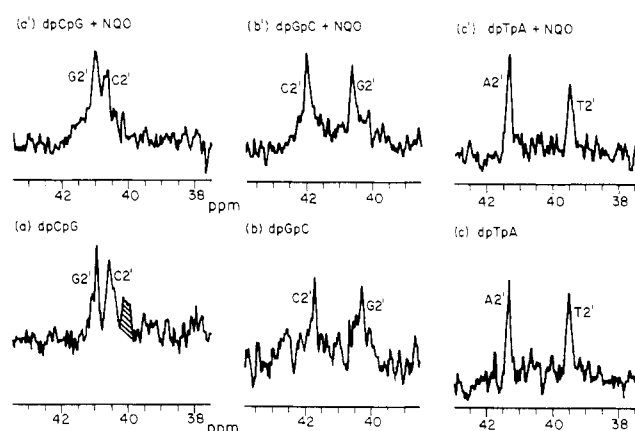FIGURE 2: ^{13}C NMR spectra of C2′ for (a) dpCpG (4.1 mM) and (a′) dpCpG (5.8 mM) [NQO (2.1 mM)], (b) dpGpC (3.7 mM) and (b′) dpGpC (5.8 mM) [NQO (1.9 mM)], and (c) dpTpA (4.0 mM) and (c′) dpTpA (5.8 mM) [NQO (2.1 mM)]. Temperature 35 °C; sodium cacodylate (0.01 M)–NaCl (0.1 M)–EDTA (0.2 mm) buffer in 25–30% D$_2$O, pH 7.0.
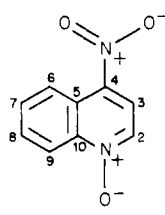
Table III: Differences in Proton Chemical Shifts between NQO Complexed with Self-Complementary Dinucleotides and Free NQO

NQO

$\delta_B - \delta_F$ (ppm)

NQO proton	dpCpG	dpGpC	dpTpA	dpApT
2	−0.11	−0.15	−0.17	−0.19
3	−0.09	−0.11	−0.16	−0.17
6	−0.11	−0.17	−0.25	−0.24
7	−0.05	−0.27	−0.17	−0.17
8	−0.12	−0.07	−0.07	−0.21
9	−0.16	−0.16	−0.20	−0.22

downfield as is shown in Figure 2. No such shifts were observed with dpTpA–NQO or dpApT–NQO mixtures. The −pN$_2$ C2′ resonances for dpCpG, dpTpA, and dpApT did not shift. However, a shift was observed for −pN$_2$ C2′ of dpGpC. With the possible exception of the C1′ resonances, no shifts were observed for the other sugar carbons. The C1′ resonances for the dpN$_1$− and −pN$_2$ sugars generally overlapped, making assignment and observation of shift changes unfeasible.

The observed chemical shifts of the NQO protons are weight averages of the chemical shifts of free and bound species. Thus, the chemical shifts of the NQO protons in the complexes with the dinucleotides were calculated in a manner similar to that used for the ^{13}C δ_B of the base carbons:

$$\delta_B = \left(\delta_{obsd} - \frac{[NQO]_T - [c]}{[NQO]_T} \delta_F \right) \frac{[NQO]_T}{[c]}$$

The δ_F values used for the NQO protons were those given previously (Winkle & Tinoco, 1978). The values of [c] were calculated by using the K values at 25 °C (Table I). In Table III the differences between the δ_B and δ_F values for the different dinucleotide:NQO complexes are presented. As expected, different patterns of shift changes are observed for the four complexes. The shift changes were compared to com-

posite ring current diagrams corresponding to a plane (3.4 Å from each base plane) in the interior of a dinucleotide minihelix.[2] As ring current effects are probably the dominant factor contributing to the NQO proton shifts in an intercalated complex, the comparison can indicate a conformation for each complex.

Discussion

Optical Studies and Equilibrium Constants. The seven dinucleotide–NQO mixtures give charge-transfer bands of similar intensities and with similar λ_{max} values. The molar absorptivities and λ_{max} values for the dinucleotide:NQO complex bands are also very close to those we observed for the 5′-mononucleotides (Winkle & Tinoco, 1978).
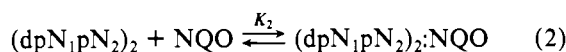
The complexes of NQO with two non-self-complementary dinucleotides form 1:1 complexes with equilibrium constants [$K(25$ °C)] of the same order of magnitude as the mononucleotides (Winkle & Tinoco, 1978). When the ability to form a minihelix is present as with the self-complementary dinucleotides and with a mixture of dpTpG and dpCpA, the complex stoichiometry is two dinucleotides to one NQO. This

[2] The diagrams were based on the calculated ring currents of Giessner-Prettre & Pullman (1970) and were constructed by T. Early, UCSD.

suggests that, in the complex, the dinucleotides form a minihelix with the NQO bound between the two dinucleotides. The experimentally determined equilibrium constants, K, are representative of the overall equilibrium

$$2dpN_1pN_2 + NQO \overset{K}{\rightleftharpoons} (dpN_1pN_2)_2 \cdot NQO$$
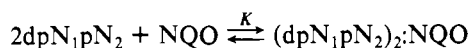
The equilibrium for the complex may be thought of as the sequence of two reactions (eq 1 and 2). The determined K

$$2dpN_1pN_2 \overset{K_1}{\rightleftharpoons} (dpN_1pN_2)_2 \qquad (1)$$

$$(dpN_1pN_2)_2 + NQO \overset{K_2}{\rightleftharpoons} (dpN_1pN_2)_2 \cdot NQO \qquad (2)$$

is then equal to the product K_1K_2. Note that the mechanism for complex formation need not necessarily be these two steps. However, by considering the complex formation in this form, the contribution of minihelix formation (reaction 1), i.e., base stacking and base pairing, to the energy of the complex may be assessed. Young & Krugh (1975) determined equilibrium constants (at 2 °C) for minihelix formation by dpGpC (K_1 = 7.8) and dpCpG (K_1 = 3.0). Equilibrium constants were not determined for dpTpA and dpApT, but for the mixed system dpApC + dpGpT much less duplex formation occurs. No dimerization of the ribodinucleoside monophosphate rApU was observed under similar conditions (4 °C) by Krugh et al. (1976), although duplex formation of rCpG and rGpC was roughly comparable to their deoxy counterparts.

Since the K values for formation of 2:1 dimer:NQO complexes are all on the order of 10^4 M^{-2} and the contributions of minihelix formation to the complex free energy are small (K_1 values are 10 M^{-1} or less), a sizable component of the complex energy is due to NQO–dinucleotide interactions (including the charge-transfer interactions). After removal of the component of the equilibrium constant due to minihelix formation, the equilibrium constants (K_2) for 2:1 complex formation from the minihelix are still 2 to perhaps 4 orders of magnitude greater than those for 1:1 dinucleotide:NQO complexing. The NQO binding affinity is thus much higher for dinucleotides capable of minihelix formation.

With certain intercalating molecules, marked sequence specificities among dinucleotides have been noted. For example, ethidium bromide shows a preference for Pyr-Pur sequence over Pur-Pyr sequences (Krugh et al., 1975; Krugh & Reinhardt, 1975). The situation with NQO is somewhat less clear. The sequence C-G seems to be preferred over G-C, especially if one considers the approximate K_2(C-G) and K_2(G-C) obtained by dividing the experimental K values by Krugh's K_1 values (which were obtained under different conditions). However it may not be true that C-G in a helix is preferred over A-T, T-A, or C-A:T-G or that Pyr-Pur sequences are in general preferred to Pur-Pyr. The similar values of K for the different dimers could indicate that NQO exhibits no distinct sequence preference for dinucleotide helixes.

NMR Studies of the Self-Complementary Dinucleotide:NQO. The information obtained from the ^1H and ^{13}C NMR studies (Tables II and III and Figure 2) was analyzed to provide structural information on the noncovalent complexes. The ring currents of the dinucleotide bases shift the NQO protons upfield. The magnitude of each upfield shift change is related to the distance of each proton from the centers of the composite ring current of the four bases. The magnitudes of all the chemical shift changes observed are somewhat diminished relative to the calculated ring current shifts; however, only the relative shifts are important for our
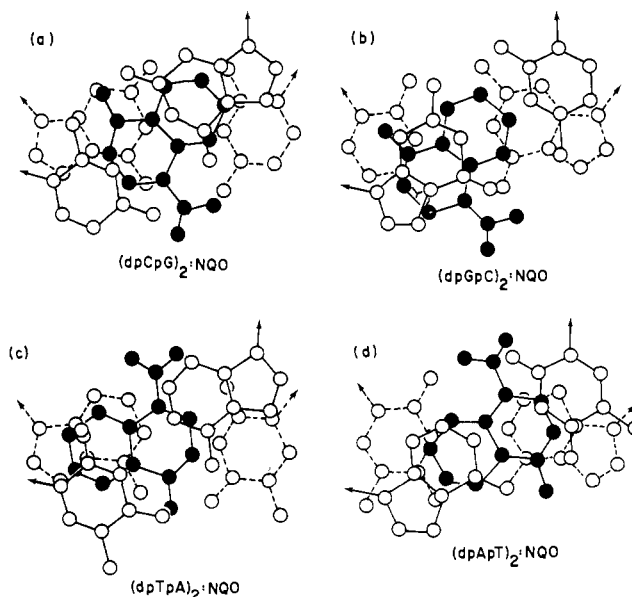

FIGURE 3: Proposed structures of self-complementary dimer:NQO 2:1 complexes. (a) (dpCpG)$_2$:NQO; (b) (dpGpC)$_2$:NQO; (c) (dpTpA)$_2$:NQO; (d) (dpApT)$_2$:NQO. Only base atoms (excluding hydrogens) are shown for the dimers. Bottom base pair (O--O); top base pair (O—O); NQO (●—●). These are approximate representations of the complex structures.

purposes. Such diminutions were also observed with the mononucleotide:NQO complexes (Winkle & Tinoco, 1978). The $\delta_B - \delta_F$ values (Table III) were compared with ring current diagrams for the four dinucleotide minihelixes. Comparisons were attempted to three different ring current diagrams corresponding to three distinct duplex orientations. In all cases the base pairs were 6.8 Å apart. The first orientation was with the dinucleotide minihelix corresponding to a B DNA structure, that is, with one base pair rotated by 36° with respect to the other. The second orientation had a 10° rotation rather than 36°; this corresponds to a 26° unwinding (Wang, 1974). The third orientation was a 10° rotation of one base pair and a 1 Å displacement of the bottom base pair. In this orientation one base pair is lined up more or less directly over the other, whereas in the first two cases the base pairs are staggered. This last orientation is what has been suggested for ethidium intercalation by Sobell et al. (1976). For all four dinucleotides, the best fits were with the base pairs at 36°.

Complexes in which the NQO is intercalated with its long axis roughly perpendicular to the long axis of the base pairs may be ruled out. In such complexes, the NQO protons H2,3 and/or H7,8 would be far removed from the ring current center. The ring current shift changes $\delta_B - \delta_F$ would be near zero for these protons in such conformations. As is shown in Table III, for all four systems all protons have $\delta_B - \delta_F$ values of the same order of magnitude.

The approximate complex orientations obtained are given in Figure 3 (parts a–d); it is clear that they represent an average of a dynamic situation. In the (dpCpG)$_2$:NQO and (dpGpC)$_2$:NQO complexes, the electron-withdrawing ring of the NQO (the NO$_2$, NO ring) is closer to the imidazole ring of the guanine. The NO$_2$ group of NQO is near the G6 carbonyl and C4 amino groups in what could be termed the major groove. The NO group of NQO is near the G2,C2 area.

With the (dpTpA)$_2$:NQO and (dpApT)$_2$:NQO complexes, it is the benzenoid ring of the NQO which is to the side of the intercalation pocket near the imidazole ring. The NO$_2$, NQO ring is in the center of the pocket, over the six-membered rings of the purine bases. The NO$_2$ group projects near the A2

hydrogen and T2 carbonyl into what may be called the minor groove.

In making the comparisons, we made the assumption that NQO forms a distinct type of complex with each dinucleotide rather than a range of very different complex structures. If NQO intercalated to form a variety of complexes with each dimer, the differences in $\delta_B - \delta_F$ in Table III for the different NQO protons would tend to disappear. For example, if NQO formed either a complex with its nitro group in the major groove or a complex with its nitro group in the minor groove (in other words, came in from either side) and took up the same position relative to one of the purines, the $\delta_B - \delta_F$ values for H2 and H3 would be very similar to those for the pairs H7 and H8 and H6 and H9. As the data show, this is not the case. Furthermore, formation of unique complexes with dinucleotides has been observed with other molecules such as ethidium bromide (Jain et al., 1977), 9-aminoacridine (Sakore et al., 1977), and proflavine (Neidle et al., 1977). The fit of the data for dpTpA, and to a lesser degree for dpApT, was not as good as those for dpCpG and dpGpC. This could indicate that there is slippage of the NQO in the intercalation pockets of dpTpA and dpApT duplexes. The proposed structures would allow for this since the NQO is in the center of the intercalation site—with the dpGpC and dpCpG complexes it is to one side. (Note that the self-complementary dimers possess a twofold axis of symmetry. Thus, the complex with the NQO stacked with one purine is identical with that with the NQO stacked in a similar manner with the other purine.)

The ^{13}C NMR study of the dinucleotide base carbons provided data which can be interpreted in terms of the complex structures. The changes arising in δ_{B1} and δ_{B2} for each type of base carbon are due primarily to the ring current of the intercalated NQO and to a lesser extent to the ring current of the other bases. In addition, there are effects from changes in the local atomic anisotropy (local paramagnetic term) due to charge transfer, hydrogen bonding, etc. The ring current effect will produce upfield shift changes (Giessner-Prettre & Pullman, 1970), whereas the charge transfer from the bases apparently produces downfield changes. The more an individual carbon is involved in the electron transfer, the larger the shielding changes are. This can be rationalized in terms of current theories of ^{13}C shielding parameters (Karplus & Pople, 1963; Cheney & Grant, 1967). In a previous paper (Winkle & Tinoco, 1978), we discussed the ^{13}C NMR spectra of dpG–NQO and dpA–NQO mixtures. In the dpG–NQO case, a large downfield shift was observed for G8 relative to the other guanine base carbons. This suggested that the electron-withdrawing center (the NO_2, NO ring) of NQO was over the imidazole ring of the guanine. With dpA–NQO no such large shifts were observed for any adenine carbon, suggesting that the NQO electron-withdrawing ring was more located over both rings of adenine.

With all the dinucleotides, the ^{13}C shift changes were smaller than was observed with the mononucleotides. In the dinucleotide:NQO complexes, the charge transfer can involve *four* bases and the NQO. Thus, the effect of the charge transfer is diminished. This is especially true when the withdrawing "center" is not over one end of the molecule, such as the imidazole ring of the purines. Furthermore, as δ_B is the average of δ_{B1} and δ_{B2}, a shift of δ_{B1} and δ_{B2} in opposite directions will also diminish its magnitude.

With the dimer dpGpC the carbons of the imidazole ring of the guanine, G5, G8, and G4, show relatively large downfield shift changes; C6 and C5 of cytosine show smaller

downfield shifts. This is consistent with having the electron-withdrawing ring of NQO, the NO_2, NO ring, over the imidazole ring of one of the guanines with a lesser interaction with C5, C6. With the dimer dpCpG, only C5 of the non-base-pairing carbons shows a downfield shift. However C6 shows a smaller upfield change than other carbons in dpCpG. This suggests that the widthdrawing NQO ring is over these regions. The differences in shift changes between the two sequences dPur-Pyr and dPyr-Pur are explained by the conformations of the stacked dimers. With dPur-Pyr dimers the imidazole ring is exposed, while in dPyr-Pur dimers it is covered partially by the dpN_1-sugar. Similarly, in the dPur-Pyr dimers the pyrimidine residue is partially blocked by the dpN_1-sugar. More overlap by the intercalator with the imidazole ring is therefore possible in the dPur-Pyr sequence.

With dpApT, much smaller shift changes are seen than with dpGpC and the pattern is different. With dpGpC, the changes on the guanine were in the order G5 > G4 $\simeq$ G8. With dpApT, the order was A4 > A8 > A5, and A5 exhibited an upfield change. The changes on the pyrimidine carbons 5 and 6 were much less downfield with dpApT than with dpGpC. The preferred position of the NO_2, NO ring may be over the center of the dpApT duplex. Similarly with dpTpA, A4 is shifting less upfield than are A5 and A8. This is also consistent with placing the NO_2, NO ring over the center of the duplex as the ^1H NMR data suggest.

The dpN_1-sugar 2' carbons of both of the dimers dpCpG and dpGpC showed downfield shifts. Such downfield shifts could be caused by the proximity of the NQO molecule. In such a position, the 2' carbons are in the downfield shielding region of the NQO ring current. This is consistent with the orientations proposed in parts a and b of Figure 3, in which the NQO is to the side of the intercalation pocket. With dpApT and dpTpA no shifts of the dpN_1 2' carbons were observed. In the duplexes formed by these two dimers, the NQO is in the center of the pocket.

The orientations which the NQO assumes relative to the guanine residues in the dpGpC and dpCpG complexes are close to the orientation which NQO has with the mononucleotide. Also, the NQO orientation in the dpApT and dpTpA complexes resembles the orientation in the NQO:dpA complex.

Conclusions

Analyses of charge-transfer spectral data for different dinucleotide–NQO mixtures have provided equilibrium constants and stoichiometries for their complexes. The preference of NQO is for dimers which form miniature double strands. No marked sequence specificity was noted among the dimers examined. Results of investigations of DNA–NQO interactions now under way in our laboratory indicate the possibility of specificity for some larger structural feature or sequence.

From the NMR studies, structures for NQO:self-complementary dimer complexes are proposed. With each dimer, NQO assumes a specific orientation. The structures of the dpCpG complex and the dpGpC complex are similar, as are those for the dpTpA complex and the dpApT complex. The orientations which NQO assumes in the noncovalent complexes may be of importance in determining the structure of the covalent adducts.

References

Benesi, H. A., & Hildebrand, J. H. (1949) *J. Am. Chem. Soc.* *71*, 2703.

Cheney, B. V., & Grant, D. M. (1967) *J. Am. Chem. Soc.* *89*, 3319.

Giessner-Prettre, C., & Pullman, B. (1970) *J. Theor. Biol.* *27*, 87.

Jain, S. C., Tsai, C.-C., & Sobell, H. M. (1977) *J. Mol. Biol.* *114*, 317.

Karplus, M., & Pople, J. A. (1963) *J. Chem. Phys. 38*, 2803.

Krugh, T. R., & Reinhardt, C. G. (1975) *J. Mol. Biol. 97*, 133.

Krugh, T. R., Wittlin, F. N., & Cramer, S. P. (1975) *Biopolymers 14*, 197.

Krugh, T. R., Laing, J. W., & Young, M. A. (1976) *Biochemistry 15*, 1224.

Nagata, C., Kodama, M., Tagashira, Y., & Imamura, A. (1966) *Biopolymers 4*, 409.

Neidle, S., Achari, A., Taylor, G. L., Berman, H. M., Carrell, H. L., Glusker, J. P., & Stallings, W. C. (1977) *Nature*

(*London*) *269*, 304.

Ochiai, E. (1953) *J. Org. Chem. 18*, 534.

Okano, T., Niitsuma, A., Takadata, A., & Uekama, K. (1969a) *Gann 60*, 97.

Okano, T., Uekama, K., & Taguchi, E. (1969b) *Gann 60*, 295.

Okano, T., Takadata, A., & Kano, T. (1969c) *Gann 60*, 557.

Okano, T., Maenosono, J., Tetsuya, K., & Onoda, I. (1973) *Gann 64*, 227.

Sakore, T. D., Jain, S. C., Tsai, C.-C., & Sobell, H. M. (1977) *Proc. Natl. Acad. Sci. U.S.A. 74*, 188.

Sobell, H. M., Tsai, C.-C., Gilbert, S. G., Jain, S. C., & Sakare, T. D. (1976) *Proc. Natl. Acad. Sci. U.S.A. 73*, 3068.

Wang, J. C. (1974) *J. Mol. Biol. 89*, 783.

Winkle, S. A., & Tinoco, I., Jr. (1978) *Biochemistry 17*, 1352.

Young, M. A., & Krugh, T. R. (1975) *Biochemistry 14*, 4841.

Kinetics of Hydrogen–Deuterium Exchange in Guanosine 5′-Monophosphate and Guanosine 3′:5′-Monophosphate Determined by Laser-Raman Spectroscopy[†]

M. J. Lane and G. J. Thomas, Jr.*

ABSTRACT: Pseudo-first-order rate constants governing the deuterium exchange of 8-CH groups in guanosine 5′-monophosphate (5′-rGMP) and guanosine 3′:5′-monophosphate (cGMP) were determined as a function of temperature in the range 30–80 °C by means of laser-Raman spectroscopy. For each guanine nucleotide the logarithm of the rate constant exhibits a strictly linear dependence on reciprocal temperature: i.e., $k_\psi = A e^{-E_a/RT}$ with $A = 8.84 \times 10^{14}$ h^{-1} and $E_a = 24.6$ kcal/mol for 5′-rGMP and $A = 3.33 \times 10^{13}$ h^{-1} and $E_a = 22.2$ kcal/mol for cGMP. Exchange of the 8-CH groups in guanine nucleotides is generally 2–3 times more rapid than in adenine nucleotides [cf. G. J. Thomas, Jr., & J. Livramento (1975) *Biochemistry 14*, 5210–5218]. As in the case of adenine nucleotides, cyclic and 5′ nucleotides of guanine exchange at markedly different rates at lower temperatures, with exchange in the cyclic nucleotide being the more facile. Each of the guanine nucleotides was prepared in four different isotopic modifications for Raman spectral analysis. The Raman frequency shifts resulting from the various isotopic substitutions have been tabulated, and assignments have been given for most of the observed vibrational frequencies.

In previous work from this laboratory (Thomas & Livramento, 1975) laser-Raman spectroscopy was used to determine the pseudo-first-order rate constant (k_ψ) governing the exchange in neutral D$_2$O solution of hydrogen by deuterium at the position 8 carbon of the adenine ring. Values of k_ψ, accurate to within 5%, were determined over the temperature range 30–90 °C for adenosine 5′-monophosphate (5′-rAMP), adenosine 3′:5′-monophosphate (cAMP), and polyriboadenylic acid [poly(rA)].

The plot of k_ψ vs. the reciprocal temperature was strictly linear only for 5′-rAMP in the cited temperature interval. Above 60 °C exchange in cAMP approached that of 5′-rAMP. Below 50 °C, however, exchange in cAMP was considerably faster than in 5′-rAMP. The exchange kinetics thus indicate that below 50 °C the nucleotides 5′-rAMP and cAMP are electronically dissimilar or are subject to associative interactions which differ in such a way that the lability of the 8-CH bond is significantly affected. It was not clear from the information obtained previously (Thomas & Livramento, 1975) whether 5′-rAMP should be regarded as the norm and cAMP

as anomalously rapid with respect to 8-CH exchange or, conversely, whether exchange in 5′-rAMP is likely to have been retarded due to associative interactions, e.g., base stacking. Exchange in poly(rA) was found to be greatly retarded compared with either of the adenine nucleotides, a result which is expected in view of the polynucleotide secondary structure.

In order to gain further insight into the role of the cyclic ribosyl phosphate moiety on the kinetics of 8-CH exchange in the attached purine and to complete a systematic study of exchange in the common purine ribonucleotides, we have investigated the rates of deuterium exchange of 8-CH groups in guanosine 5′-monophosphate (5′-rGMP) and guanosine 3′:5′-monophosphate (cGMP). Quantitative Raman spectroscopy was again used to determine both the exchange rate constants over the temperature range 30–80 °C and the related Arrhenius activation energy, E_a, and frequency factor, A, in the expression shown in eq 1.

$$\ln k_\psi = \ln A - E_a/RT \qquad (1)$$

The results obtained here are compared with those obtained previously on corresponding adenine nucleotides to reveal the extent to which different substituents at the C(2) and C(6) purinic ring positions affect the lability of the 8-CH group in the imidazole heterocycle. Analogous rate constant determinations were not made for poly(rG) because of the well-known aggregation of this polynucleotide and the problems